TÜBİTAK

Turkish Journal of Earth Sciences

http://journals.tubitak.gov.tr/earth/

Research Article

Turkish J Earth Sci
(2019) 28: 85-102
© TÜBİTAK
doi:10.3906/yer-1802-24

Miocene sediment mineralogy of the lower Chelif basin (NW Algeria): implications for weathering and provenance

Fatiha HADJI[1], **Abbas MAROK**[1,*], **Ali MOKHTAR SAMET**[2]

[1]Department of Earth and Universe Sciences, University of Tlemcen, Tlemcen, Algeria
[2]Department of Hydraulics, University of Chlef, Chlef, Algeria

Received: 23.02.2018 • **Accepted/Published Online:** 26.11.2018 • **Final Version:** 15.01.2019

Abstract: Mineralogical investigations of clay and nonclay minerals were conducted on the Miocene sediments from three sections of the lower Chelif basin, northern Algeria. Bulk rock analyses of Miocene sediments show that these clastic sediments are dominated by variable mineralogical compositions and concentrations. Quartz is the dominant mineral through the three stratigraphic intervals and calcite (except in the upper layers) and dolomite are lacking in the Messinian deposits. The clay mineralogy is dominated by smectite (24%) and mixed-layer illite-smectite (I-S) (22%) during the Burdigalian-Langhian, illite (36%) and kaolinite (28%) in the Tortonian, and illite (49%) and I-S (20%) in the Messinian stratigraphic range. The smectite-(kaolinite+chlorite)-illite ternary diagram shows that, in general, Miocene sediments originated from a mixed mafic and felsic source and were influenced by physical erosion and chemical weathering processes.

Key words: Burdigalian-Langhian, Tortonian, Messinian, clay minerals, nonclay minerals

1. Introduction

Differences in the composition of clay minerals and their relative abundances are related to climatic conditions (humidity and temperature) and geological factors such as lithology, and they can reflect paleoenvironmental conditions (e.g., climate, tectonic activity, and burial diagenesis) (Chamley, 1989; Velde, 1995; Bolle and Adatte, 2001; Garzanti et al., 2004; Wang et al., 2011; Dera et al., 2009 ; Liu et al., 2012). Their mineralogical analysis constitutes a powerful tool for understanding paleoclimate and paleoweathering conditions in a source area (Chamley et al., 1989; Ahlberg et al., 2003; Dera et al., 2009; Rostási et al., 2011; Singh et al., 2016; Hassan, 2017: Li et al., 2017).

Among these minerals, illite and chlorite are generally inherited from parent rocks by physical erosion under low-hydrolysis conditions where chemical weathering of mafic minerals and feldspars is limited (Weaver, 1989; Rostási et al., 2011).

Illite and chlorite are considered to be the dominant clay minerals of soils that have undergone weak chemical weathering (Robert and Kennet, 1994). They are characteristic of cold regions (Bockheim, 1982) and deserts (where low temperatures and/or low rainfall reduce chemical weathering) as well as high-relief areas where erosion limits soil formation, especially during periods of intense tectonic activity (Biscaye, 1965; Millot, 1970; Chamley, 1998; Robert and Kennett, 1994).

In general, kaolinite develops in well-drained continental areas that are characterized by high rainfall and leaching of parent rocks (Robert and Chamley, 1991), leading to alkaline and alkaline-earth element removal (Millot, 1970). Kaolinite can result from weathering of K-feldspars, muscovite, and mica chemical weathering under intense hydrolysis conditions (Hu et al., 2014) as well as from increased erosion during sea-level (regression and transgression) changes (Robert and Kennett, 1994; Chamley, 1998; Thiry, 2000). Deep burial diagenesis can affect clay minerals (e.g., kaolinite can disappear under increased burial temperature at depths greater than 2000 m) (Weaver, 1989; Chamley, 1998).

Smectite minerals are usually formed under relatively warm and humid climatic conditions where moderate hydrolysis takes place (Chamley, 1989) and are a characteristic of a volcanic source (Rao and Rao, 1995).

Mixed-layer illite-smectite (I-S), one of the most frequently observed clay minerals in sedimentary sequences (Weaver, 1989), can be formed by mineralogical transformation of illite under low temperatures due to repeated wetting and drying of soils (Singer, 1988) and may occur as a result of diagenetic alteration of smectite

* Correspondence: a_marok@yahoo.fr

This work is licensed under a Creative Commons Attribution 4.0 International License.

to illite (Rostási et al., 2011). According to Chamley (1998), illite, I-S, and chlorite associated with quartz and feldspars are considered as terrigenous species. In marine sediments, illite occurrence is generally related to detrital processes (Rateev et al., 1969).

The present study examines the detailed mineralogy of the Miocene sediments of the Algerian margin (lower Chelif basin, northern Algeria) and attempts to constrain their chemical weathering and provenance. It completes the results obtained on clay and nonclay minerals in the Mediterranean basins, in particular Miocene basins of Morocco, Tunisia, France, and Spain. Three representative sections of the northern and southern margins of the basin were selected for this purpose.

2. Geological setting and stratigraphic context

During the last decades, many geological studies (e.g., sedimentology, paleontology, tectonics) have been made in the lower Chelif basin (Perrodon, 1957; Mazzola, 1971; Delfaud et al., 1973; Tauecchio and Marks, 1973; Delteil, 1974; Guardia, 1975; Fenet, 1975; Bizon and Bizon, 1976; Meghraoui, 1982, 1986; Rouchy, 1982; Rouchy et al., 2007; Thomas, 1985; Belkebir, 1986; Saint-Martin, 1987; Neurdin-Trescartes, 1992, 1995; Ameur-Chehbeur, 1988; Belkebir et al., 1996, 2002; Bessedik et al., 2002; Aïfa et al., 2003; Atif et al., 2008; Belhadji et al., 2008; Mansour et al., 2008; Arab et al., 2015). This 100-km-long basin belongs to the sublittoral Neogene basins of northwestern Algeria. It is located between the littoral massifs (Murdjadjo, Orousse, and Dahra) in the north and the Tessala Mountains, Ouled Ali, Béni Chougrane, and Ouarsenis in the south (Figure 1a). It is characterized by Mio-Plio-Quaternary sediments discordant over a Mesozoic basement (Cretaceous schist) (Figure 1b) containing alkaline and calc-alkaline rocks (Perrodon, 1957; Aïfa et al., 1992).

In this basin, the lower Miocene facies record important changes in space and time. The sedimentary sequence, which is mostly marine, is constituted by bluish marls that laterally change to sandstones, purple hard marls, and conglomerates (e.g., Perrodon, 1957; Bessedik et al., 2002). According to studies of Neurdin-Trescartes (1992, 1995) and Arab et al. (2015), the marine lower Miocene was deposited during a compressional episode in a piggyback position on top of the still-moving Tellian allochthon.

The Middle Miocene deposits consist of conglomerates, sandstones, and blue or gray marls attributed to the Langhian (Belkebir et al., 1996). This set is overlain by gray marls, marls, sandstones, reds clays, and conglomerates of the Serravallian (Bessedik et al., 2002).

Finally, for the Upper Miocene (Tortonian-Messinian), the northern and southern margins of the Chelif basin are distinguished by both marine and continental sedimentation (blue marls, diatomites, and evaporites) showing a significant variation in thickness.

In the present study, three sections were investigated on the northern (Ouillis and Amarna) and southern (Tiraouet) margins of the basin (Figure 1a).

2.1. Tiraouet section

The Tiraouet section is located southeast of Chlef village (ex. El Asnam), around 15 km north of Sendjas (Figure 1a). This section consists of marls assigned to the lower Miocene (Burdigalian) by Perrodon (1957) and to the uppermost Burdigalian-Langhian by Bessedik et al. (2002) (Figure 1b). The association of planktonic foraminifera is represented by the *Globigerinoides trilobus* and *Globoquadrina baroemoensis* species, which confirm the Burdigalian-Langhian age. The studied section is 73 m thick (Figures 2a and 2b) and consists of:

-blue marls (39 m thick) changing to sandy marls to the top. This stratigraphic interval is overlain by a tephra bed that is 0.80 m thick (Figure 2c).

-purple hard marls (34 m thick) without macrofossils overlain by a conglomerate bar.

2.2. Ouillis section

This northern section is located in the southwestern part of the Dahra massif, north of Sidi Bel Attar (Figure 1a). Taken at the Ouillis quarry, this section is represented by the upper part of the diatomite formation (19 m), which can be subdivided into two lithologically distinct units (Figure 3a), Member A and Member B.

Member A (14 m thick) is represented by centimetric to decimetric alternating layers largely dominated by the diatomite facies. From bottom to top (Figure 3b):

-9 m of dilated and monotonous alternation of diatomites and marls, with 10 cm of tephra bed at the base. The massive, centimeter-to-decimeter diatomite beds are white in color. The base and top of these beds are beige and more or less marly. The marls (0.15 to 0.70 m thick) are massive and lenticular, brown at their base to black, and grading gradually to diatomites. Samples collected from this section have a siliceous microfauna represented by radiolarians (Mokhtar Samet, 2013).

-5 m of 11 closely alternating sequences including laminated diatomite-marls and laminated diatomite-marls-gypsum. Gray laminated diatomites sometimes contain fish scales. Marls are black and 0.10 to 0.70 m thick, sometimes having laminar structures. There are five intervals of gypsum each 1 to 2 cm thick.

Member B (5 m thick) is characterized by a rhythmic alternation of marls and diatomite beds (Figure 3c). It ends with centimeter-scale limestone beds incised into the underlying marls. In the Ouillis section, the diatomite formation age was based on micropaleontological arguments and lithostratigraphic correlations with neighboring regions (Mokhtar Samet, 2013). From this point of view, a single association of benthic foraminifera could be defined towards the top of the study section

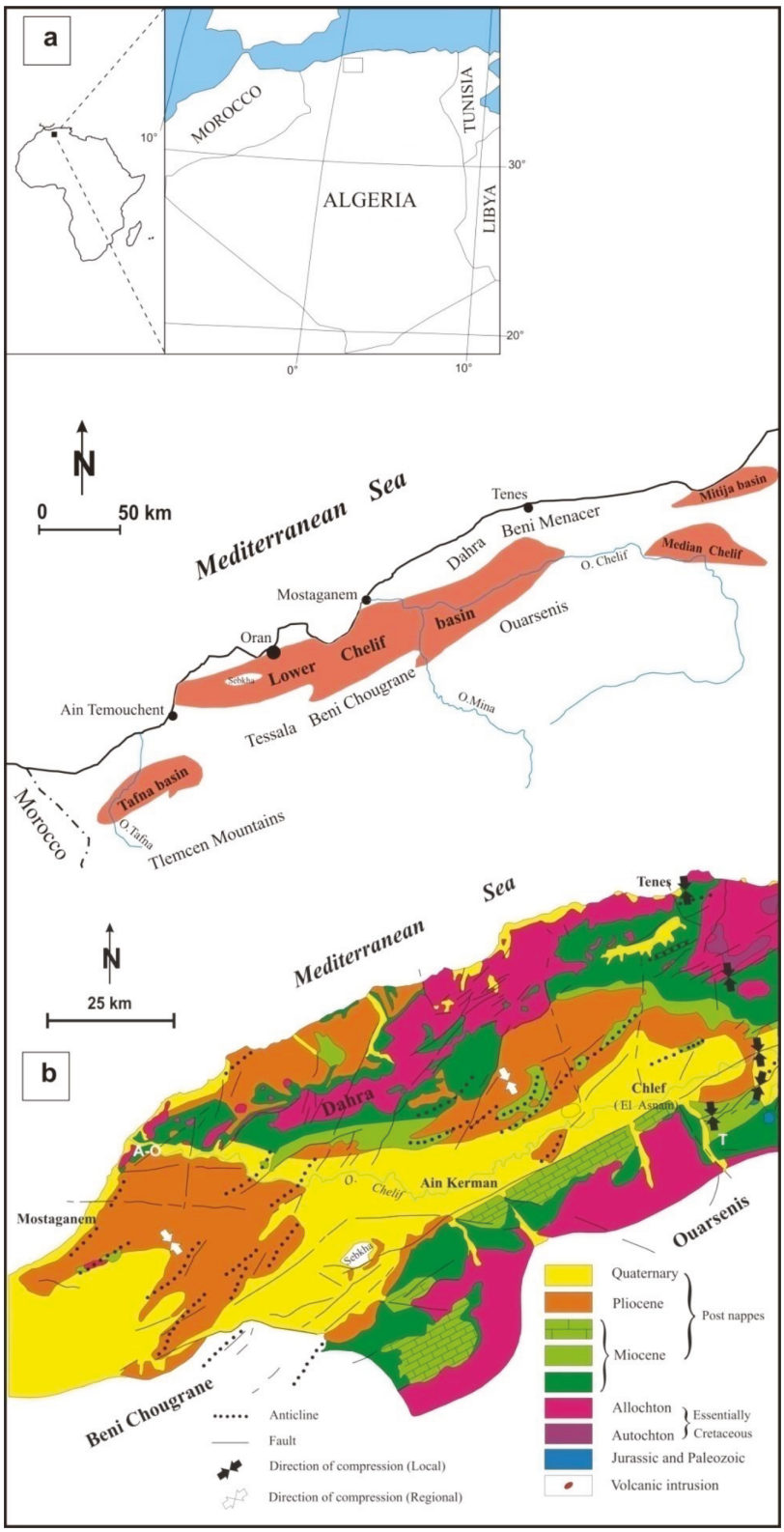

Figure 1. Geographic and geological sketch. a) Map of the Chelif Basin through the Miocene with location of the studied section (modified from Rouchy et al., 2007). b) Geological and tectonic map of the lower Chelif Basin. (A) Amarna section, (O) Ouillis section, (T) Tiraouet section (after Meghraoui, 1986).

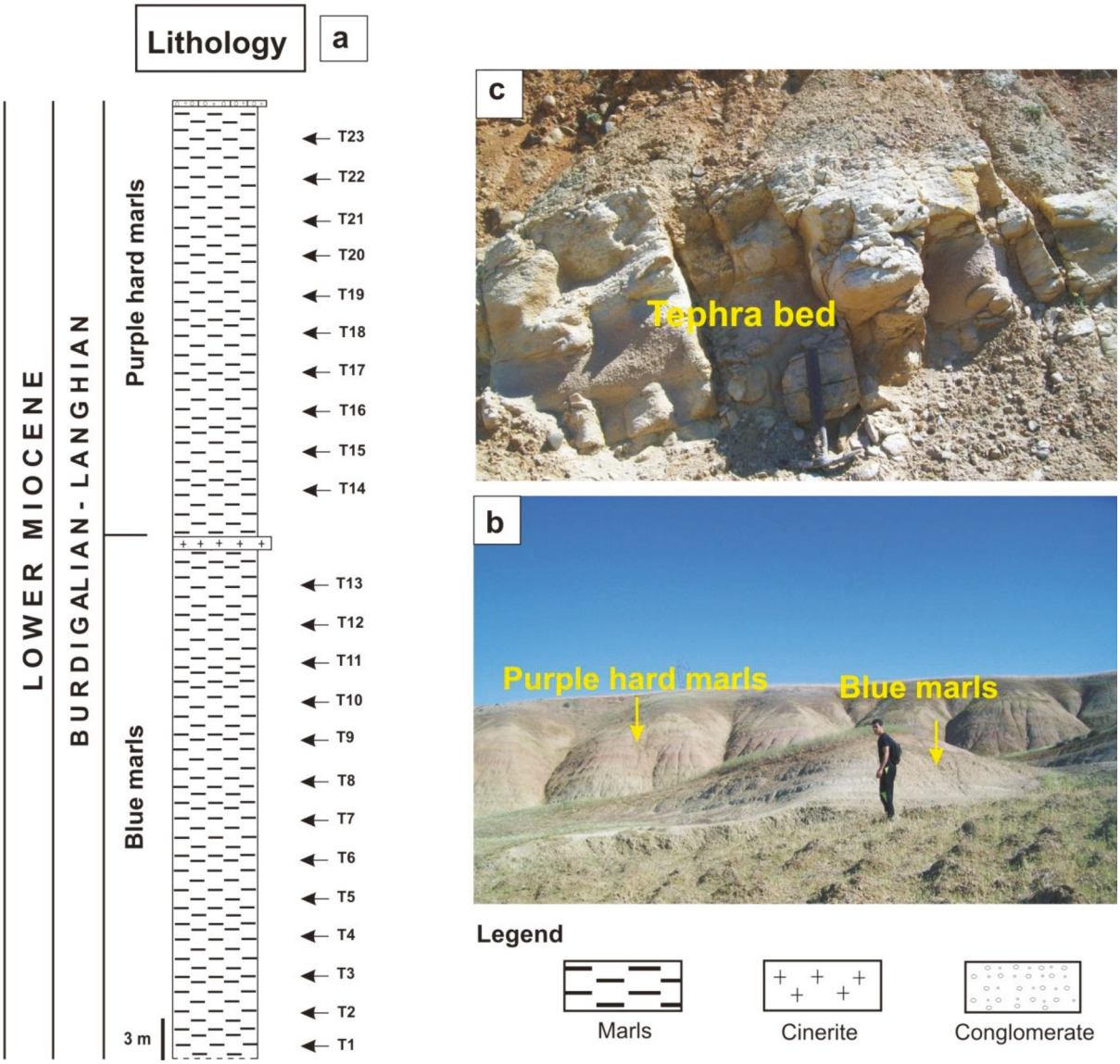

Figure 2. a) Stratigraphic columns of Tiraouet section; b) Burdigalian-Langhian layers of Tiraouet section; c) Tephra bed of Tiraouet section.

(Member B). It is composed of the following species: *Bulimina subulata*, *Bulimina aculeata*, *Bolivina dilatata*, *Bolivina dentellata*, *Uvigerina* sp., and *Rectuvigerina cylindrica*. This association gives a Messinian age (biozone *Globorotalia mediteranea*) correlating with neighboring regions. In addition, Member A, which does not contain foraminifera, can be dated by correlation with diatom assemblages in the neighboring regions (Mansour et al., 2008). The correlation confirms the Messinian (Upper Miocene) chronological interval.

2.3. Amarna section

The Amarna section is located northeast of Djebel Diss, about 16 km north of Mostaganem (Figure 1a). The lithostratigraphic succession in this section includes only the Blue Marls Formation (64 m thick) (Figures 4a and 4b). It consists of yellowish sandy marls at the base and blue marls at the top. The planktonic association represented mainly by *Neogloboquadrina acostaensis*, *Globorotalia scitula*, *Globigerinoides obliquus*, *Globigerinoides trilobus*, and *Globigerina bulloides* gives a lower Tortonian age (biozone *Neogloboquadrina acostaensis*). The same age was given by Belhadji et al. (2008). This stratigraphic interval is capped by a 0.30-m-thick conglomerate bar.

3. Materials and methods

The results presented in this study are based on the processing and analyses of 47 samples of marl layers taken

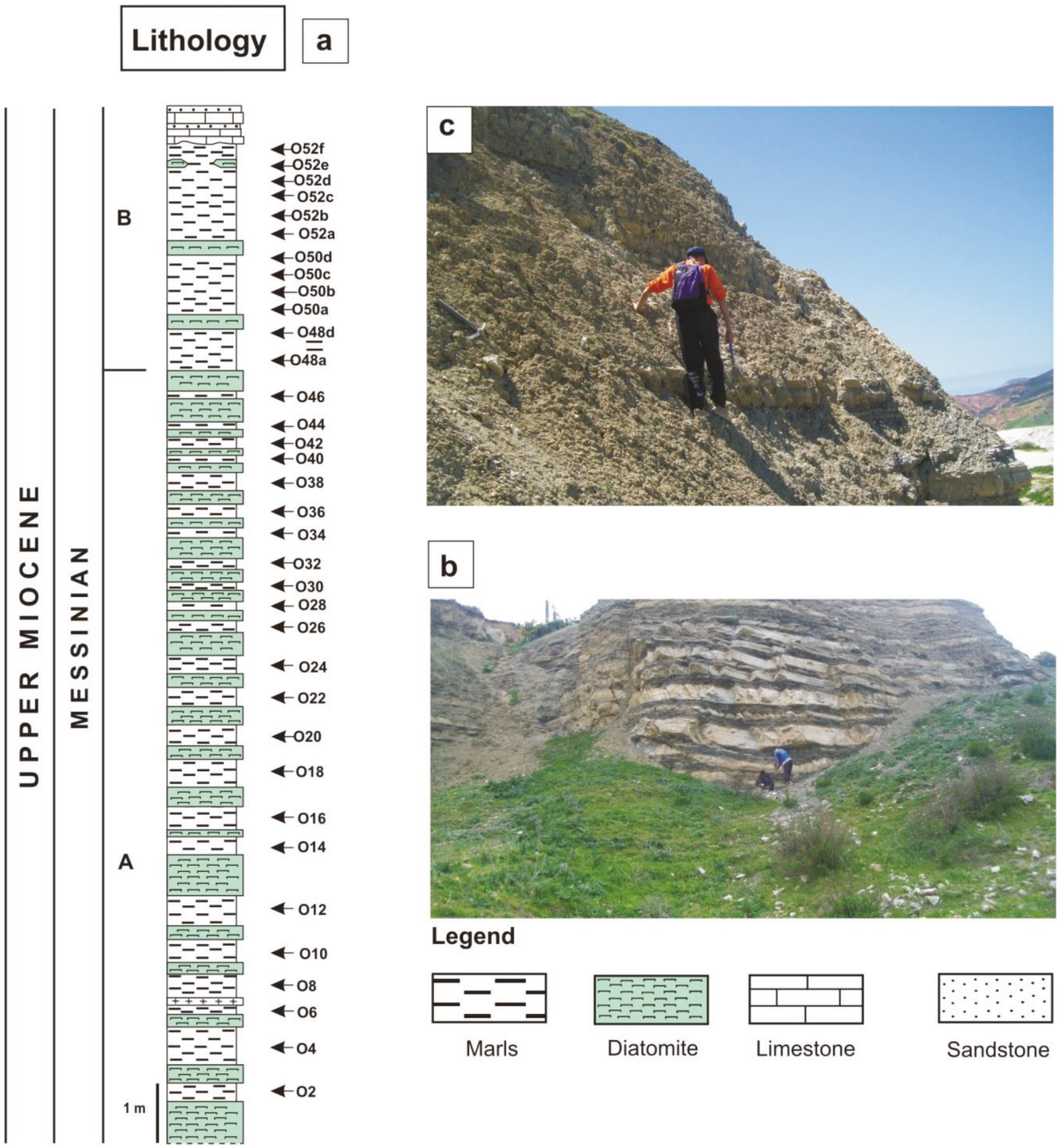

Figure 3. a) Stratigraphic columns of Ouillis section, b) Member A, c) Member B.

from Tiraouet (23), Ouillis (17), and Amarna (7) (Figures 2a, 3a, and 4a). X-ray diffraction identification of the crystalline phases was carried out on whole-rock and clay fractions with a PANanalytical XPERT-PRO diffractometer using CuKα (1.5418 Å) radiation with a ceramic copper anticathode X-ray tube under an accelerating voltage of 45 kV and a beam current of 40 mA. The positions and intensities of the observed diffraction peaks were compared with the PDF-ICDD (Powder Diffraction File) reference files for mineralogical phase identification. The RIR (Reference Intensity Ratio) included in the HighScore Plus software of the PDF-ICDD file allows the semiquantitative estimation of the corresponding detected phases when this is required and/or possible. The fine fraction (clay minerals) was extracted by wet process after removal of materials impeding their dispersion such as organic matter and carbonates. The obtained clay suspensions were spread on suitable supports for drying. Each oriented clay preparation was studied and then, depending on the need, was subjected to a heat treatment at 550 °C for 1

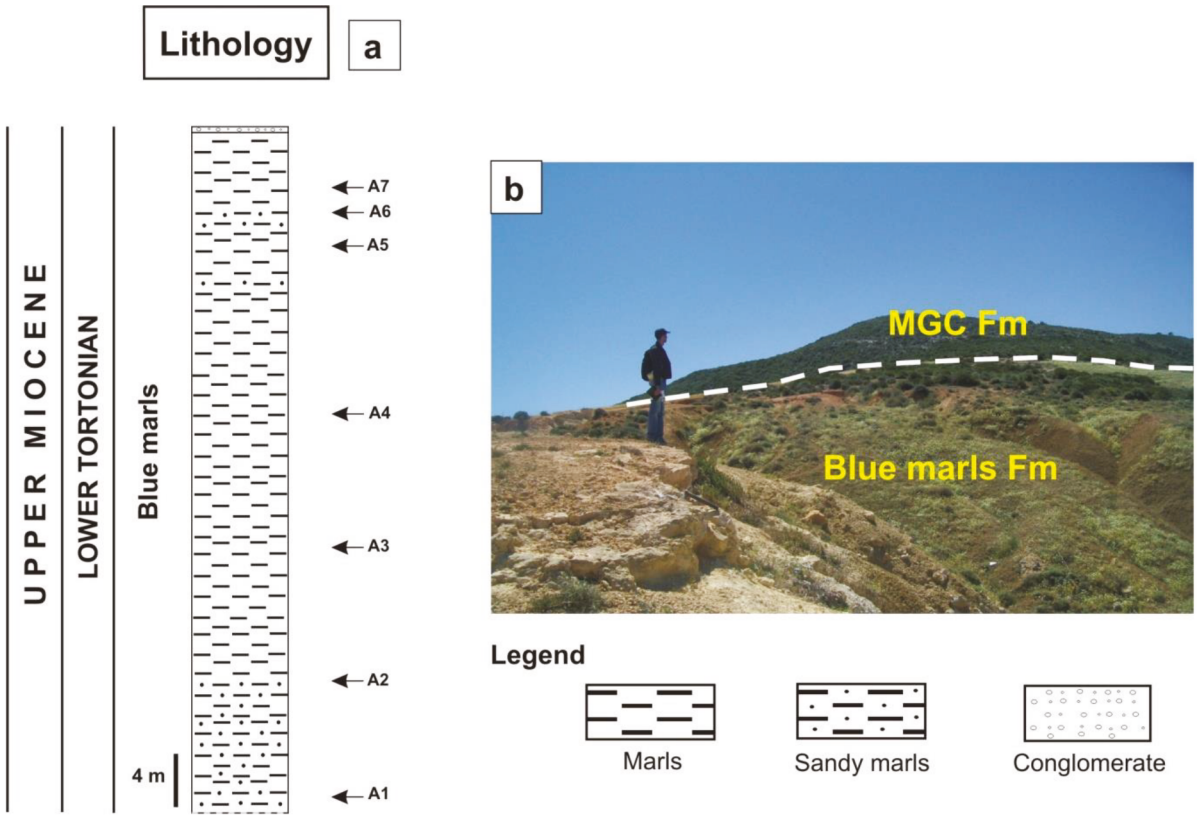

Figure 4. a) Stratigraphic columns of Amarna section, b) Blue Marls and MGC (Marls including Gypsy-Calcareous) limit of Amarna section.

h (heated clay) and/or swelling test with ethylene glycol (glycolic clay) in order to differentiate and estimate the encountered clay mineralogical phases. Abundance of clay minerals is reported in weight percent.

4. Results and interpretation

4.1. Bulk mineralogy

Table 1 shows the proportions of nonclay minerals for the Miocene sediments of the Chelif basin**.**

Bulk rock analyses of the Burdigalian-Langhian samples collected in Tiraouet show that these clastic sediments are dominated by variable concentrations of quartz (50%–65%; average: 58.4%), calcite (5%–13%; average: 8.7%), plagioclase (2%–6%; average: 3.8%), dolomite (1%–6%; average 3%), and orthoclase (2%) in the T_9-layer (Figure 5a). Pyrite (1%–2%) and halite (1%) are present only in the B-member of the Tiraouet section (Figure 5b).

For the Amarna section, concentrations of quartz in the lower Tortonian interval (A_1–A_6) are higher (61%–69%) than those of the upper one, A_7–A_8 (25%–34%). Inversely, calcite concentrations are lower (7%–13%) at the base of the section and higher (46%–65%) at the top. Dolomite is also present along this section with concentrations varying between 1% and 8%. At its base, we note the presence of plagioclase (1%–3%), anatase (1%–2%), and local orthoclase (1%–3%), gypsum (1%–2%), and siderite (trace to 1%) (Figures 5c and 5d).

At Ouillis, quartz concentrations (31%–69%; average: 59%) decrease up section and are up to 55% in almost all samples. Calcite (25%–49%) varies inversely with quartz and is observed only in the three penultimate layers of this section (Figures 5e and 5f). Dolomite is absent; plagioclase (1%–4%), orthoclase (1%–2%), and baryte (2%) are locally observed. Gypsum (1%–6%), anatase (1%–3%), and jarosite (1%–11%) are present generally in Member A (Figure 5e). Gypsum and jarosite disappear with calcite appearance. The evaporitic minerals were probably deposited during strong evaporation under warm and arid climatic conditions (Grosjean et al., 2001).

4.2. Clay mineralogy

For mineralogical interpretations of the clay minerals we followed Chamley (1989, 1998), Weaver (1989), Robert and Chamley (1991), Deconinck and Chamley (1995), Velde (1995), Velde and Meunier (2008), and Alizai et al. (2012). Selected X-ray diffractograms are shown for the Tiraouet (Figures 5a and 5b), Ouillis (Figures 5c and 5d), and Amarna (Figures 5e and 5f) sections.

Table 1. Nonclay mineral concentrations in Miocene sediments.

Age	Samples	Quartz	Calcite	Dolomite	Orthoclase	Plagioclase	Gypsum	Halite	Pyrite	Baryte	Anatase	Jarosite	Siderite
MESSINIAN	O2	55	-	-	-	2	-	-	-	-	2	11	-
	O6	55	-	-	2	3	6	-	-	-	1	8	-
	O12	65	-	-	2	3	5	-	-	-	1	2	-
	O18	64	-	-	1	3	1	-	-	-	2	3	-
	O24	68	-	-	2	2	1	-	-	-	1	1	-
	O26	56	-	-	-	3	1	-	-	-	2	9	-
	O32	61	-	-	-	2	1	-	-	-	2	4	-
	O38	64	-	-	-	3	1	-	-	-	2	3	-
	O44	62	-	-	-	3	1	-	-	2	2	2	-
	O48a	67	-	-	2	3	-	-	-	-	3	-	-
	O48b	62	-	-	0	3	tr	-	-	-	3	4	-
	O50a	68	-	-	1	3	tr	-	-	2	2	0	-
	O50c	41	30	-	0	2	-	-	-	-	1	-	-
	O51	31	49	-	-	1	-	-	-	-	1	-	-
	O52a	49	25	-	1	3	-	-	-	-	0	-	-
	O52g	67	-	-	0	4	-	-	-	-	2	-	-
TORTONIAN	A1	65	8	8	1	-	-	-	-	-	-	-	-
	A2	62	9	8	0	-	-	-	-	-	1	-	-
	A3	63	7	6	1	-	2	-	-	-	1	-	tr
	A4	62	7	7	-	-	1	-	-	-	2	-	-
	A5	61	9	6	-	-	-	-	-	-	2	-	-
	A6	69	11	3	3	3	-	-	-	-	-	-	-
	A7	34	46	4	-	1	-	-	-	-	-	-	-
BURDIGALIAN-LANGHIAN	T1	50	12	3	-	3	-	-	-	-	-	-	-
	T2	52	10	3	-	3	-	-	-	-	-	-	-
	T3	53	13	2	-	3	-	-	-	-	-	-	-
	T4	59	8	2	-	4	-	-	-	-	-	-	-
	T5	58	12	2	-	3	-	-	-	-	-	-	-
	T6	60	9	3	-	4	-	-	-	-	-	-	-
	T7	61	8	2	-	5	-	-	-	-	-	-	-
	T8	54	9	2	-	4	-	-	-	-	-	-	-
	T9	54	9	4	2	5	-	-	-	-	-	-	-
	T10	61	10	4	-	5	-	-	-	-	-	-	-
	T11	65	6	2	-	6	-	-	-	-	-	-	-
	T12	65	7	2	-	6	-	-	-	-	-	-	-
	T13	57	9	4	-	4	-	-	-	-	-	-	-
	T14	54	8	4	-	3	-	-	-	-	-	-	-
	T15	60	8	5	-	3	-	-	-	-	-	-	-
	T16	56	8	6	-	4	-	-	-	-	-	-	-
	T17	64	5	2	-	4	-	-	1	-	-	-	-
	T18	61	6	1	-	3	-	-	2	-	-	-	-
	T19	61	7	2	-	3	-	1	1	-	-	-	-
	T20	58	8	6	-	4	-	-	-	-	-	-	-
	T21	60	7	4	-	3	tr	1	-	-	-	-	-
	T22	62	8	3	-	2	-	-	-	-	-	-	-
	T23	58	13	1	-	3	-	-	-	-	-	-	-

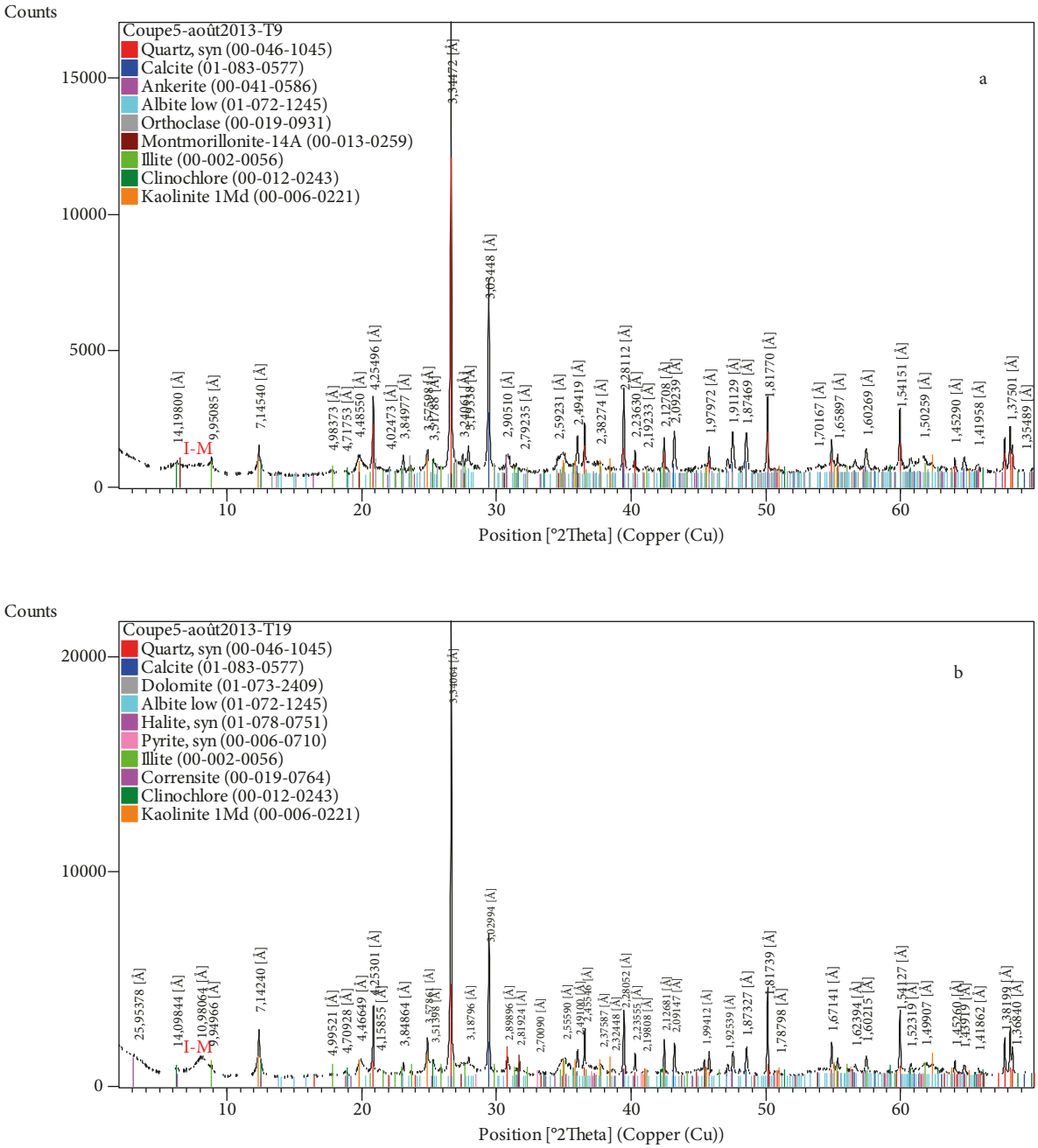

Figure 5. X-diffractograms of a) Tiraouet section (sample T_{19}), b) Tiraouet section (sample T_{21}), c) Amarna section (sample A_3), d) Amarna section (sample A_5), e) Ouillis section (sample O_{38}), and f) Ouillis section (sample O_{46}).

The clay assemblage in Figures 6a, 6b, and 6c show generally high levels of illite in the Amarna (36%) and Ouillis (49%) sections and smectite (24%) and I-S (22%) at Tiraouet.

For all the Miocene deposits, we observe an increase in illite and a decrease in chlorite from the Burdigalian-Langhian (Figure 6a) to Messinian (Figure 6b). The highest amounts of kaolinite are found in the Tortonian interval. At Tiraouet, clay minerals include smectite (15%–35%), illite (15%–30%), kaolinite (10%–20%), chlorite (10%–20%), and I-S (20%–30%) (Figure 6a). At Amarna in the Tortonian interval, the clay mineral assemblage includes smectite (0%–5%), illite (30%–55%), kaolinite (10%–50%), chlorite (0%–15%), and I-S (20%–25%) (Figure 6c).

The Ouillis section shows dominance of illite (30%–60%) and a lack of chlorite except in layer O_2 (15%). Kaolinite, smectite, and I-S percentages are 15%–20%, 0%–20%, and 15%–25%, respectively (Figure 6b).

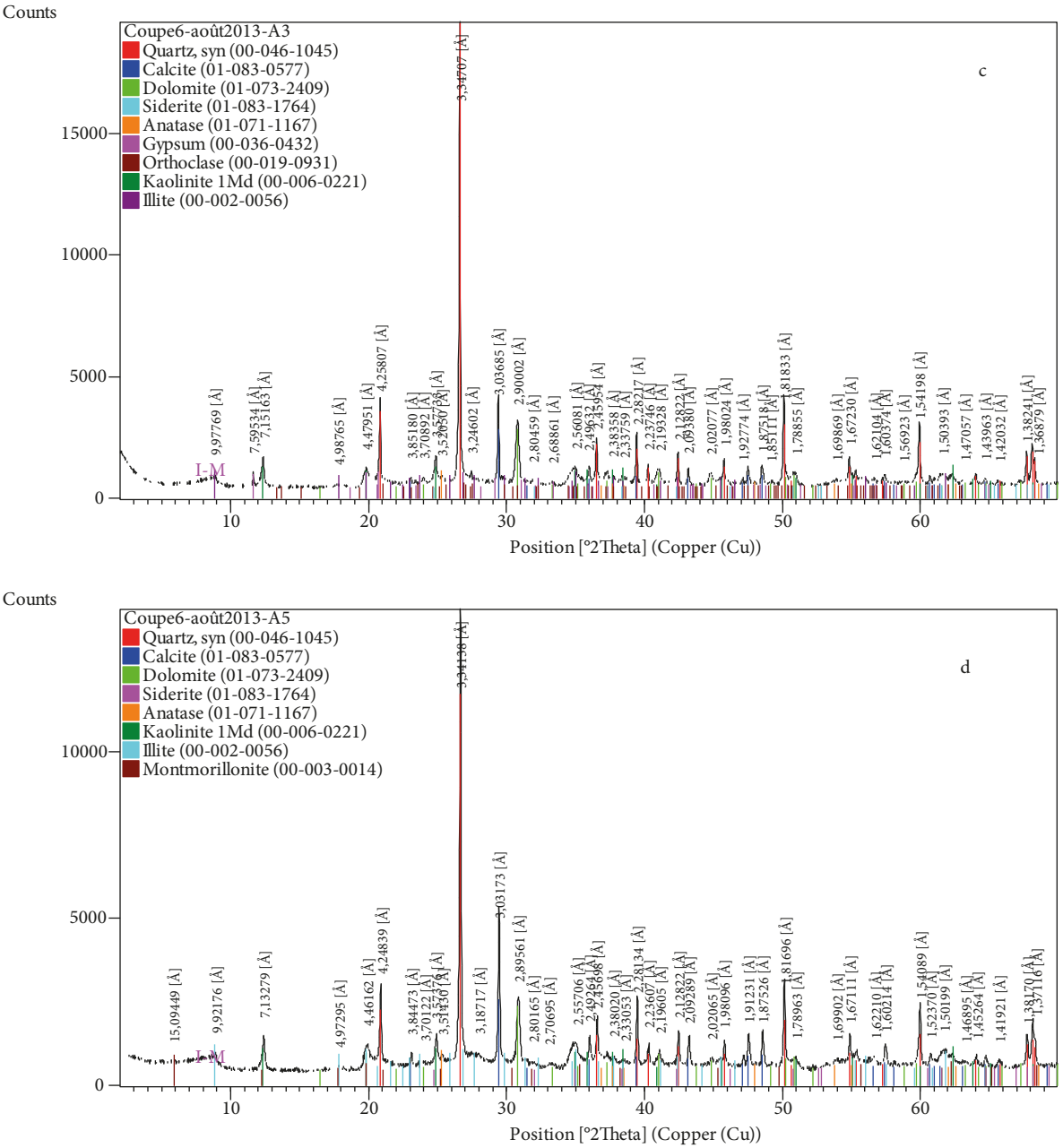

Figure 5. (Continued).

Different forcing processes (climatic, tectonic, and lithologic) play important roles in the formation and preservation of clay minerals in these study sections (Figure 7a). The smectite-(kaolinite+chlorite)-illite ternary diagram was constructed to highlight the provenance of clay minerals of Miocene sediments and their weathering types (chemical weathering and mechanical erosion) (Figure 7b). In general, this plot clearly shows that sediments originated from a mixed mafic felsic source and were influenced by both physical erosion and chemical weathering. In detail, layers of the top of the Tortonian sediments in Amarna were affected essentially by a chemical weathering process and the top by a physical erosion process (Figure 7b).

Smectite/(illite+chlorite), kaolinite/(illite+chlorite), kaolinite/smectite, kaolinite/illite, smectite/illite, and kaolinite/chlorite ratios were used in this study because they are all potentially environmentally controlled (Alizai et al., 2012) and have been used successfully in previous studies (Robert and Kennett, 1994; Alizai et al., 2012; Limmer et al., 2012; Hu et al., 2014; Li et al., 2014; Miao et al., 2016; Khonde et al., 2017). The evolving clay mineral

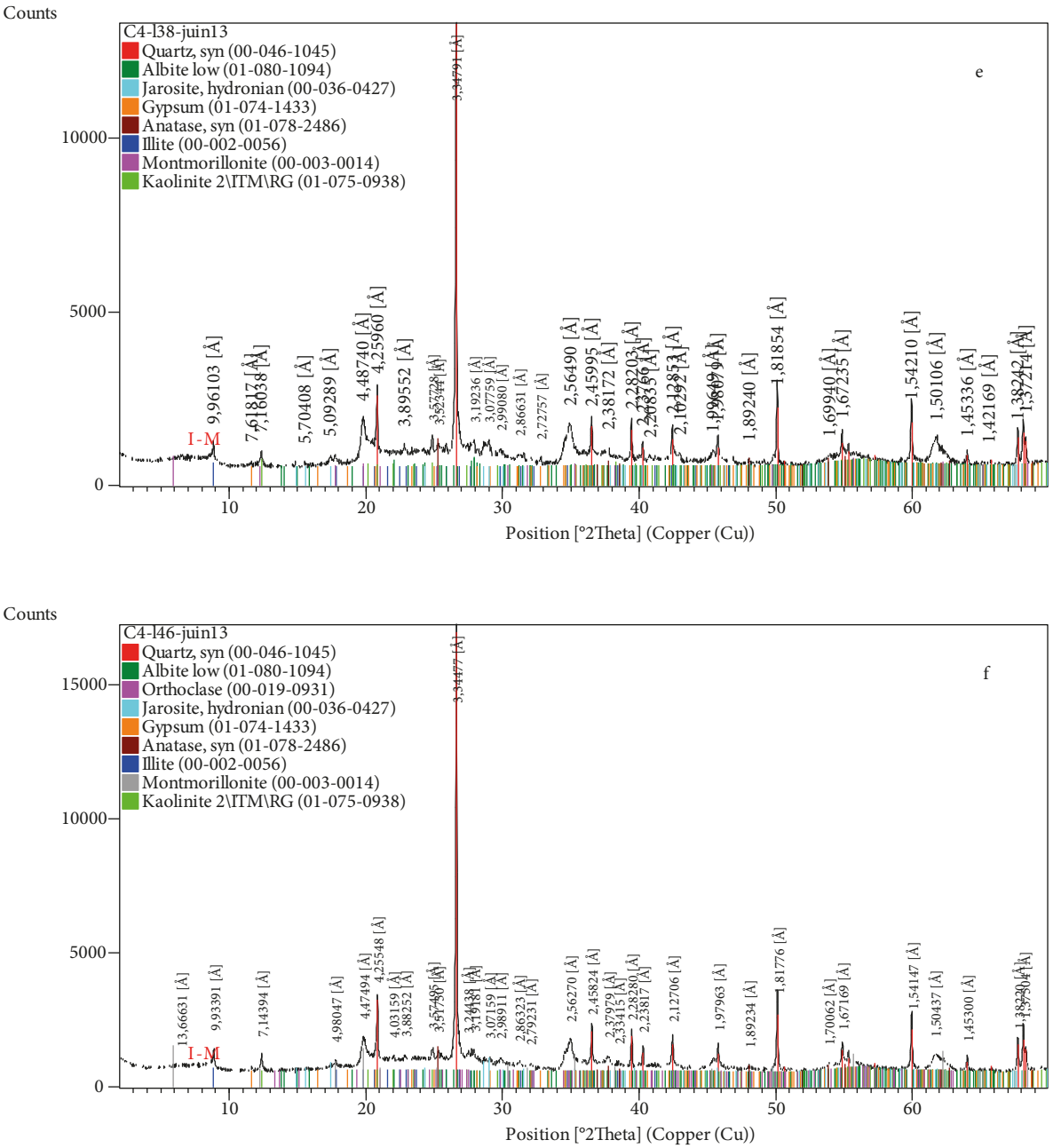

Figure 5. (Continued).

ratios in the three sections are as follows (Table 2; Figures 8a and 8b).

In the Tiraouet section (Figure 8a), for the Burdigalian-Langhian stratigraphic interval, kaolinite/smectite values are 0.33–1.33 (average: 0.72), kaolinite/illite 0.29–1.33 (average: 0.84), kaolinite/chlorite 0.5–2.0 (average: 1.06), smectite/illite 0.57–2.00 (average: 1.27), smectite/(illite+chlorite) 0.38–0.86 (average: 0.67), kaolinite/(illite+chlorite) 0.20–0.60 (average: 0.45), and (smectite+kaolinite)/(illite+chlorite) 0.60–1.67 (average: 1.09). It is noteworthy that all these ratios except smectite/illite and smectite (illite+chlorite) are generally higher in Member B at the top of the section than in Member A (Figure 8a).

For example, the chemical leaching proxy kaolinite/(illite+chlorite) averages 0.54 in Member B and 0.37 in Member A. The humidity proxies kaolinite/illite and kaolinite/chlorite behave similarly.

At Amarna (Figure 8b), kaolinite/smectite values are 7 in A_4 and 6 in A_5, whereas the kaolinite/chlorite ratio is 1.0

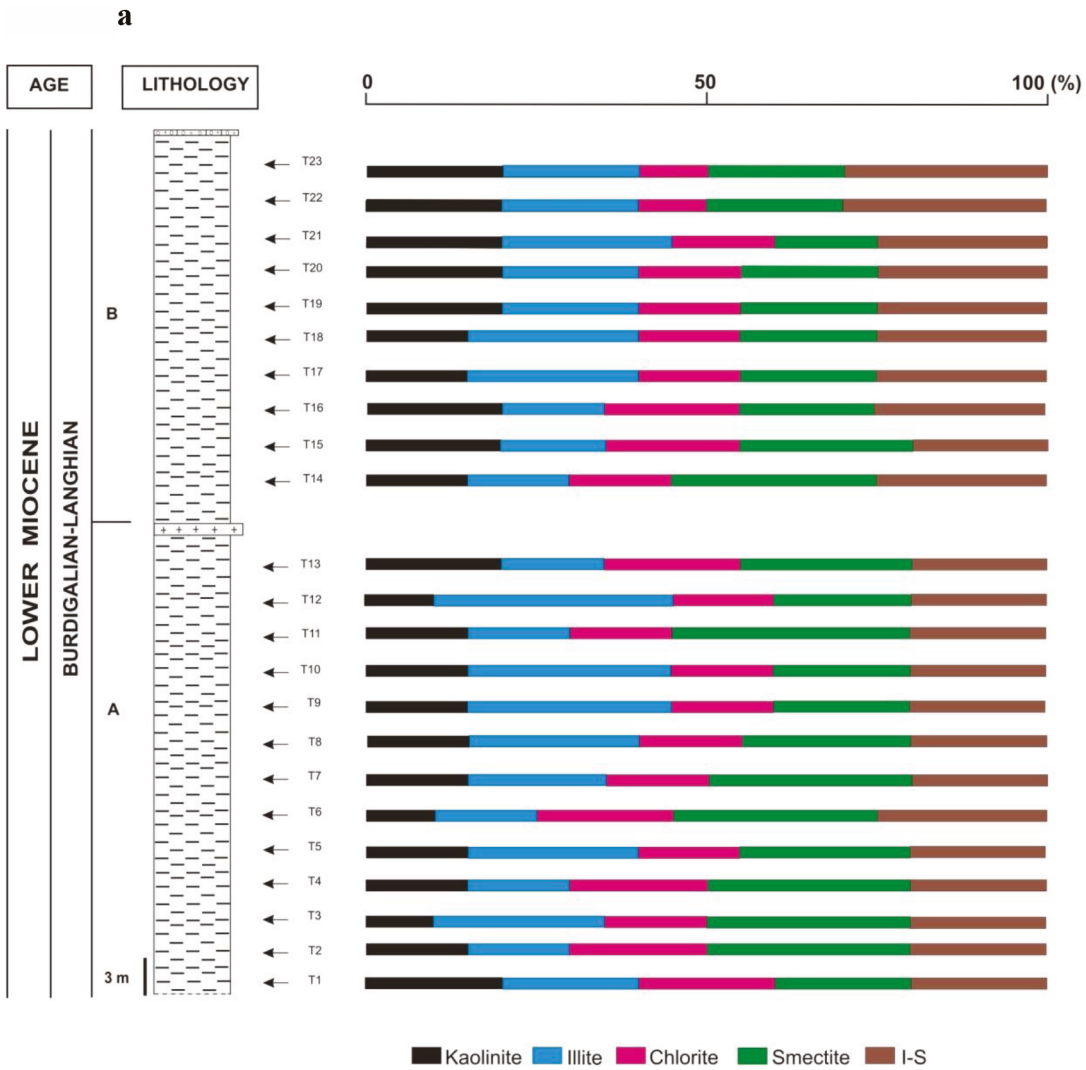

Figure 6. Relative distribution of clay minerals of Miocene sediments: a) Tiraouet, b) Amarna, and c) Ouillis.

in A_6 and A_7. Smectite/illite and smectite/(illite+chlorite) ratios show the same trends with values varying between 0.0 and 1.13 (average: 0.04). Values are 0.18–1.67 (average: 0.87) for kaolinite/illite, 0.15–1.67 (average: 0.85) for kaolinite/(illite+chlorite), and 0.15–1.67 (average: 0.89) for (smectite+kaolinite)/(illite+chlorite). These last three ratios, in contrast to smectite/(illite+chlorite) and smectite/illite, decrease from bottom to top in the Tortonian deposits.

In the Messinian stratigraphic interval (Ouillis section) (Figure 8c) values are 0–4.0 (average: 1.57) for kaolinite/smectite, 0.27–0.67 (average: 0.37) for kaolinite/illite, 0.08–0.67 (average: 0.29) for smectite/illite, 0.18–0.50 (average: 0.28) for smectite/(illite+chlorite), 0.27–0.50 (average: 0.36) for kaolinite/(illite+chlorite), and 0.42–1.00 (average: 0.48) for (smectite+kaolinite)/(illite+chlorite).

The smectite/illite, smectite/(illite+chlorite), and (smectite+kaolinite)/(illite+chlorite) ratios show a decrease from Burdigalian-Langhian sediments to Tortonian and then an increase in the Messinian. The (smectite+kaolinite)/(illite+chlorite) ratio of 0.60–1.17 (average: 0.90) suggests the dominance or equilibrium of clay minerals formed under physical erosion. Conversely, Member B shows greater values (1.00–1.67; average: 1.25), indicating the presence of clay minerals derived from chemical weathering. Kaolinite/smectite values are greater than in Member A, indicating warm and humid climatic conditions.

The kaolinite/(illite+chlorite) chemical leaching ratio and the humidity proxies kaolinite/illite and kaolinite/chlorite are high in Member B, indicating that leaching

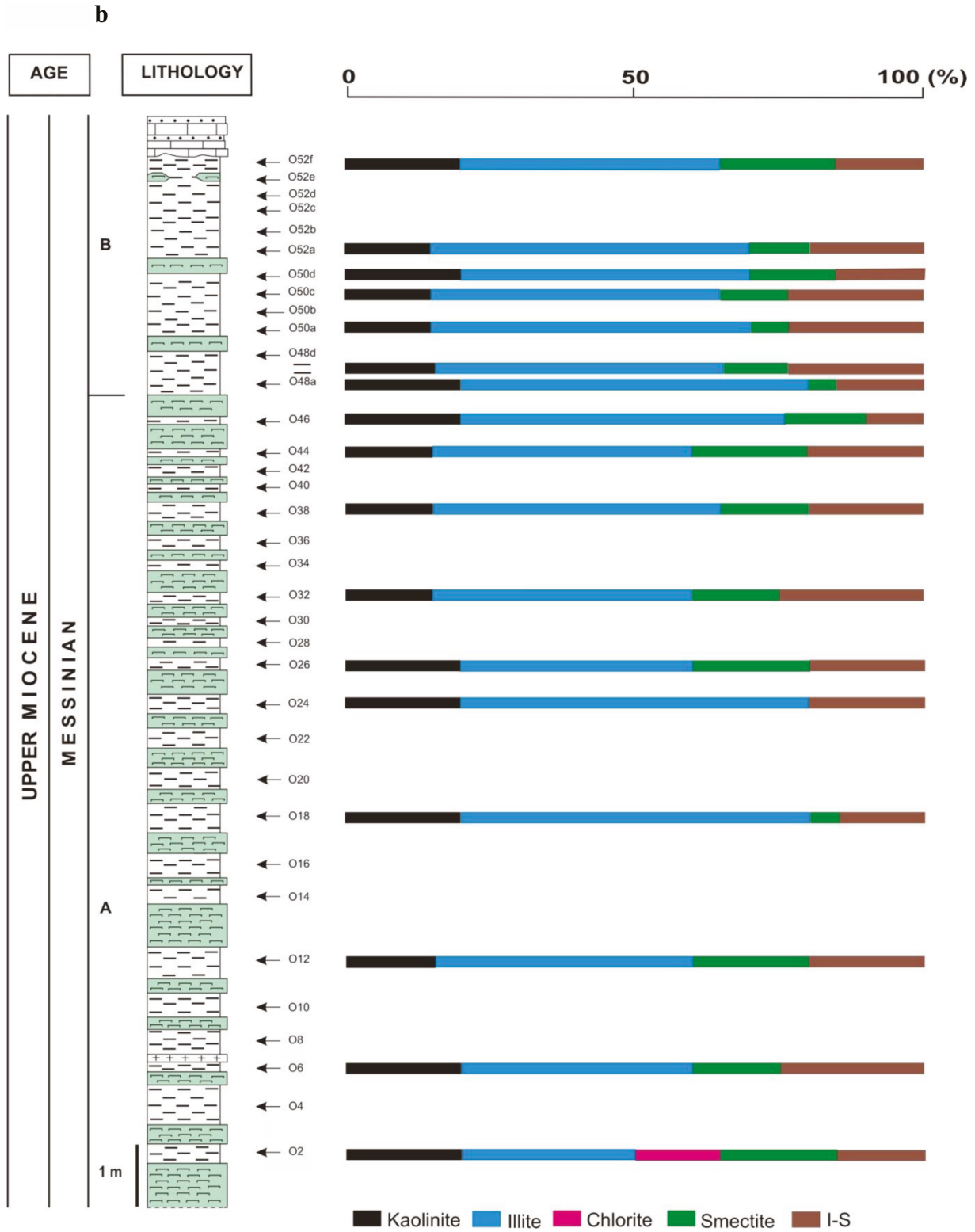

Figure 6. (Continued).

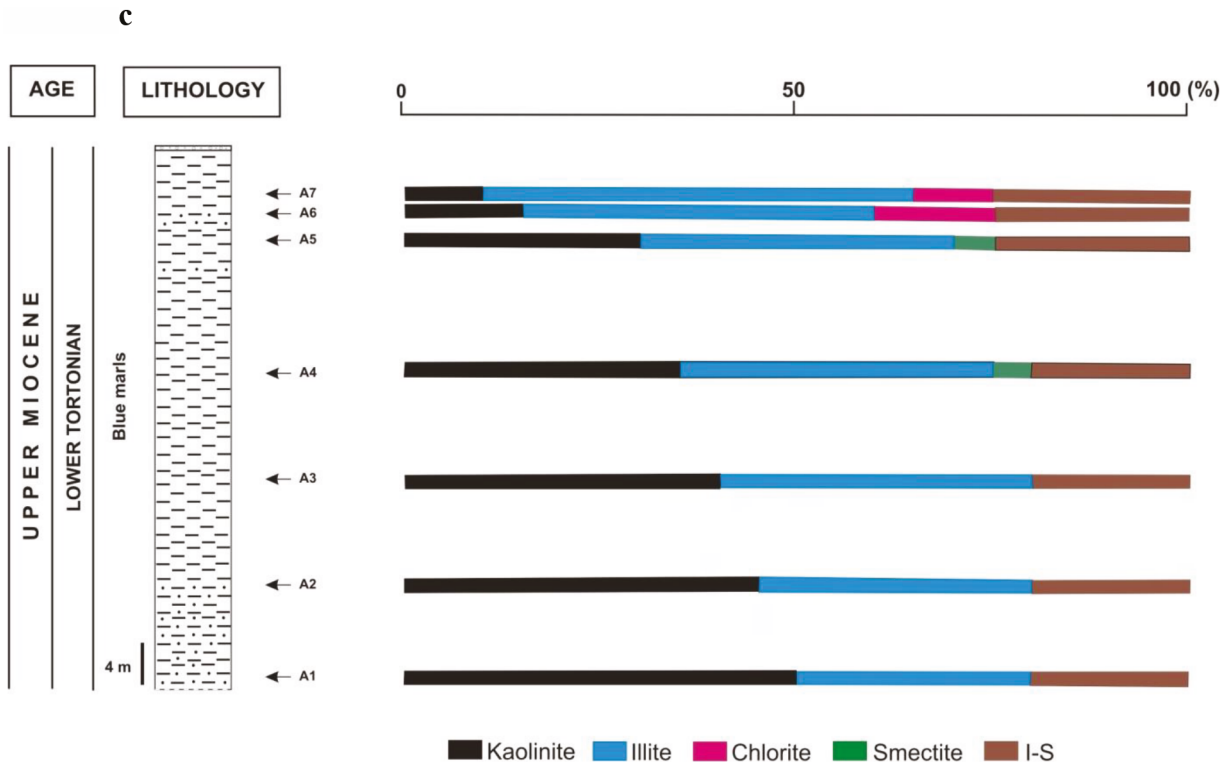

Figure 6. (Continued).

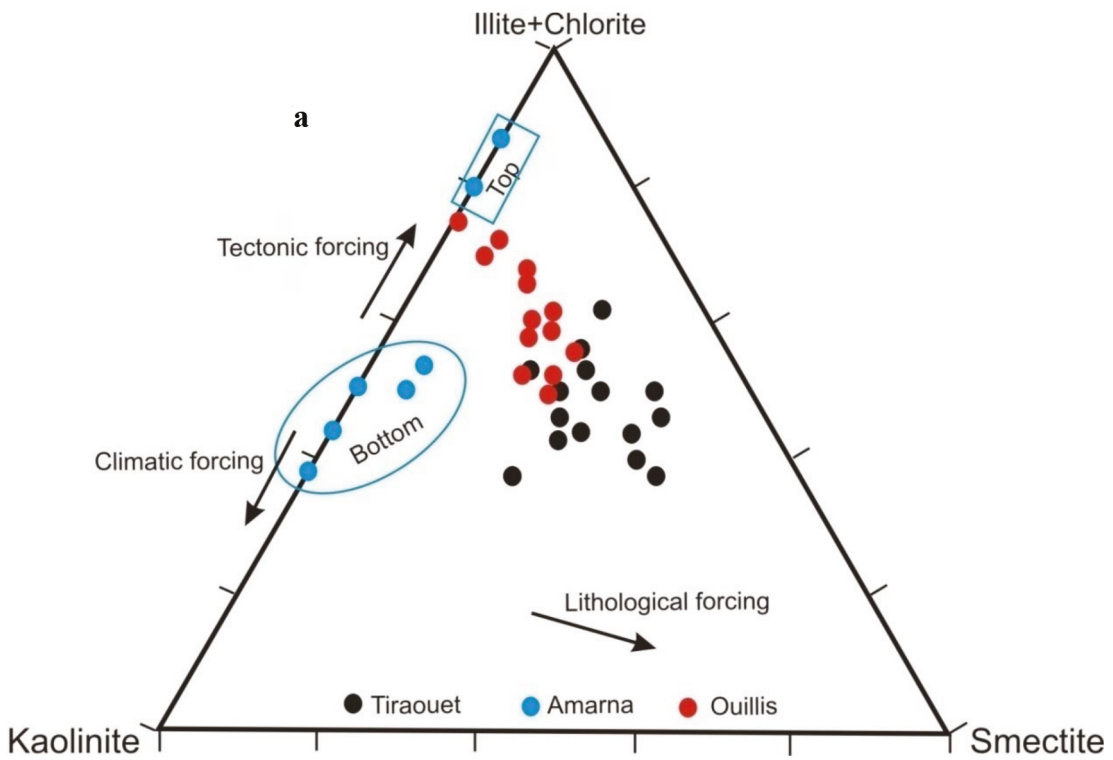

Figure 7. Ternary diagrams of the major clay mineral groups illite+chlorite, kaolinite, and smectite. (a) The principal forcing processes on clay mineral formation are also indicated (after Liu et al., 2012). (b) The provenance sources and alteration processes are also indicated (after Hu et al., 2014).

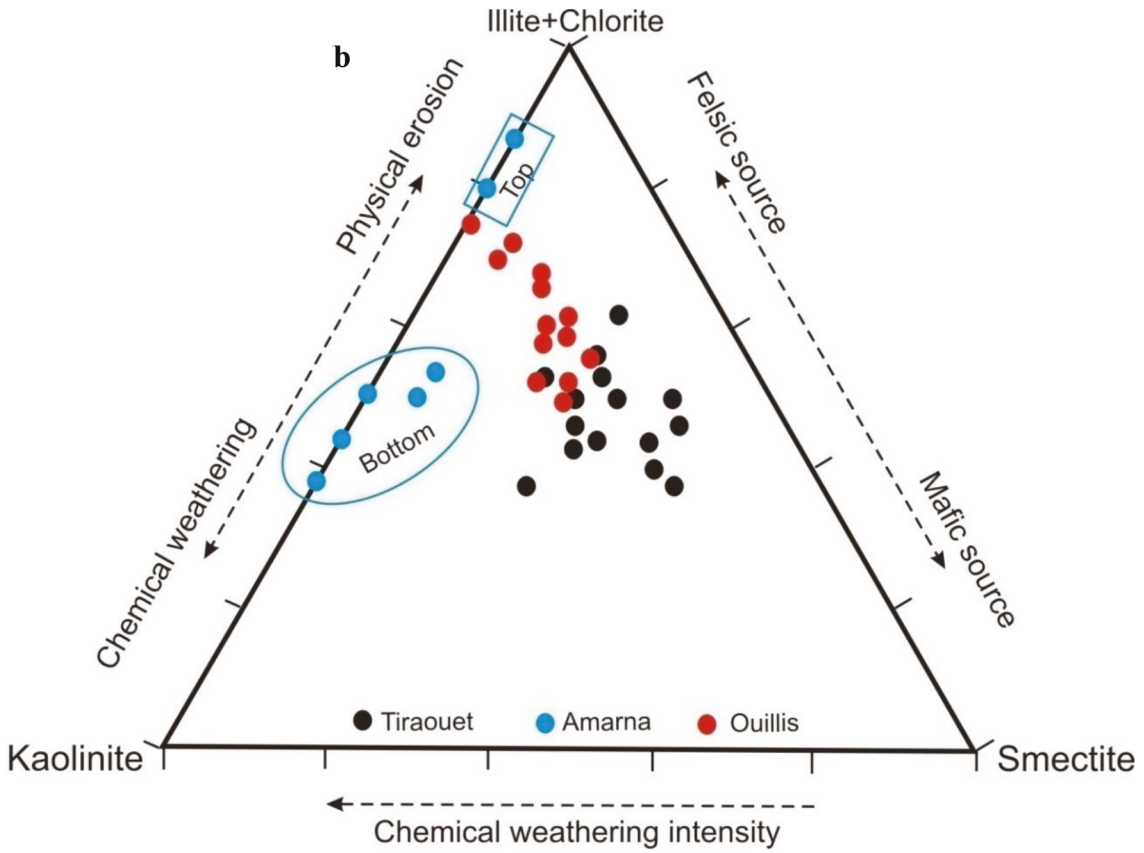

Figure 7. (Continued).

Table 2. Average values of clay ratios. G: Gypsum; H: halite, J: jarosite, B: barytine, K: Kaolinite, S: smectite, C: chlorite, I: illite, F: feldspar, Q: quartz, Ca: calcite.

Age	Member	(K+S)/(I+C)	K/(I+C)	S/(I+C)	K/I	K/C	S/I	F/Q	Ca/Q	Evap.
Messinian	A	0.82	0.58	0.32	0.40	-	0.34	0.06	0.00	G J B
	B	0.72	0.33	0.21	0.33	-	0.21	0.06	0.40	B
Tortonian	-	1.38	0.85	0.04	0.87	-	0.04	0.02	0.31	G
Burdigalian-Langhian	A	0.90	0.37	0.70	0.69	0.86	1.33	0.08	0.17	-
	B	1.25	0.54	0.64	1.00	1.25	1.20	0.06	0.13	H G (tr)

leading to kaolinite formation was more important in the upper part of the lower Miocene deposits.

5. Conclusions

The clay mineralogy of the Chelif basin Miocene sediments was investigated in three sections in order to characterize the Burdigalian-Langhian, Tortonian, and Messinian sequences and to constrain their weathering and provenance. The mineralogy reveals important variations in the concentrations of minerals. These clastic sediments are marked by variable concentrations of quartz (25%–69%) and calcite (5%–49%) and by the presence of pyrite and halite in the Burdigalian-Langhian, and by anatase and gypsum in the Tortonian and Messinian units. Barytine and jarosite were only observed in the Messinian deposits where dolomite was absent.

Clay mineral assemblages of the lower Chelif basin include illite, chlorite, kaolinite, smectite, and I/S. The Miocene sediments indicated an increase of illite from bottom (Burdigalian-Langhian) to top (Messinian) and conversely a decrease of chlorite leading to its disappearance in the Messinian unit. These sediments originated mainly from a mixed source and were influenced by physical erosion and chemical weathering processes.

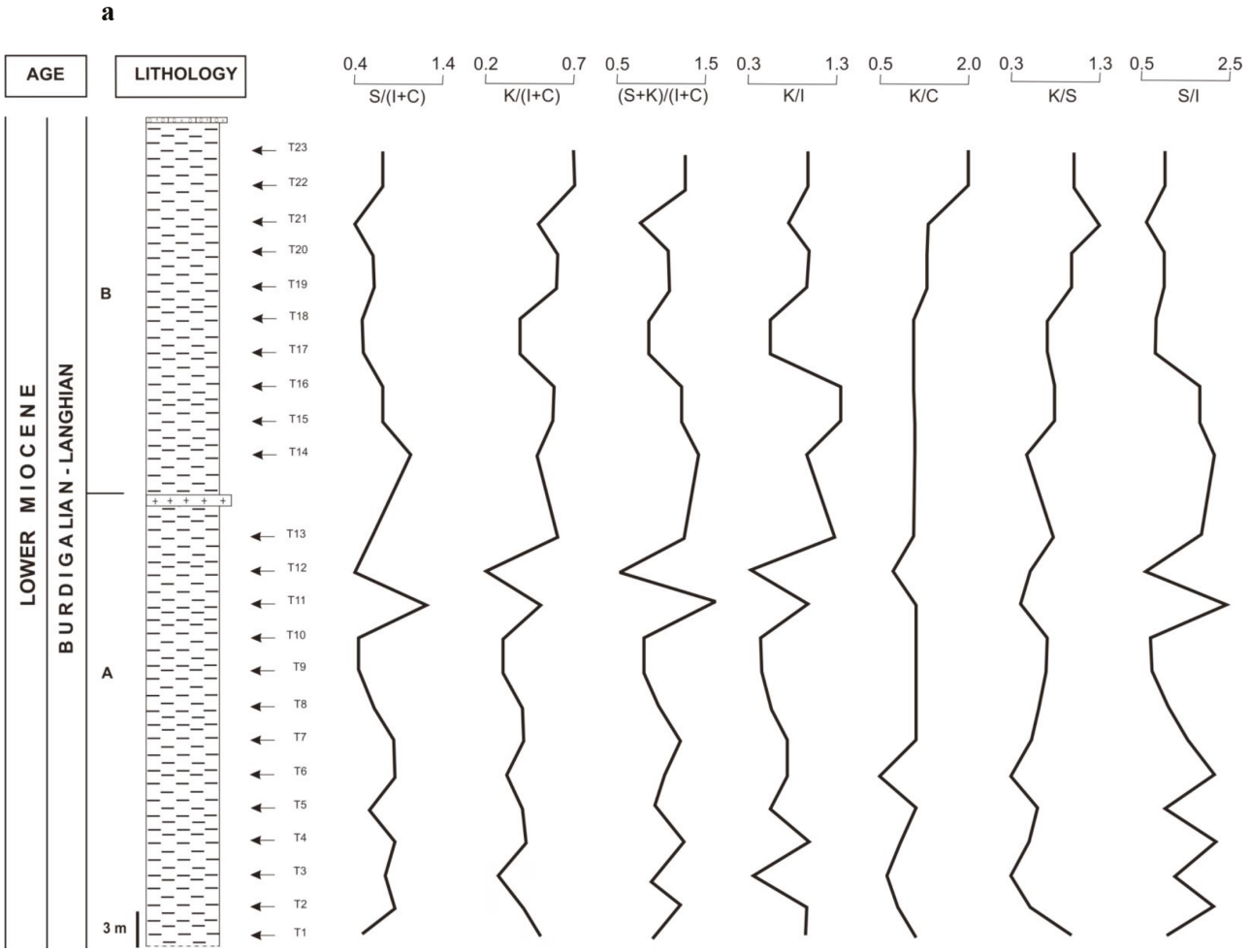

Figure 8. Variations in climate-sensitive proxy ratios: smectite/(illite+chlorite), kaolinite/(illite+chlorite), kaolinite/illite, kaolinite/smectite, kaolinite/chlorite, smectite/illite, and (smectite+kaolinite)/(illite+chlorite) of (a) Tiraouet, (b) Amarna, and (c) Ouillis.

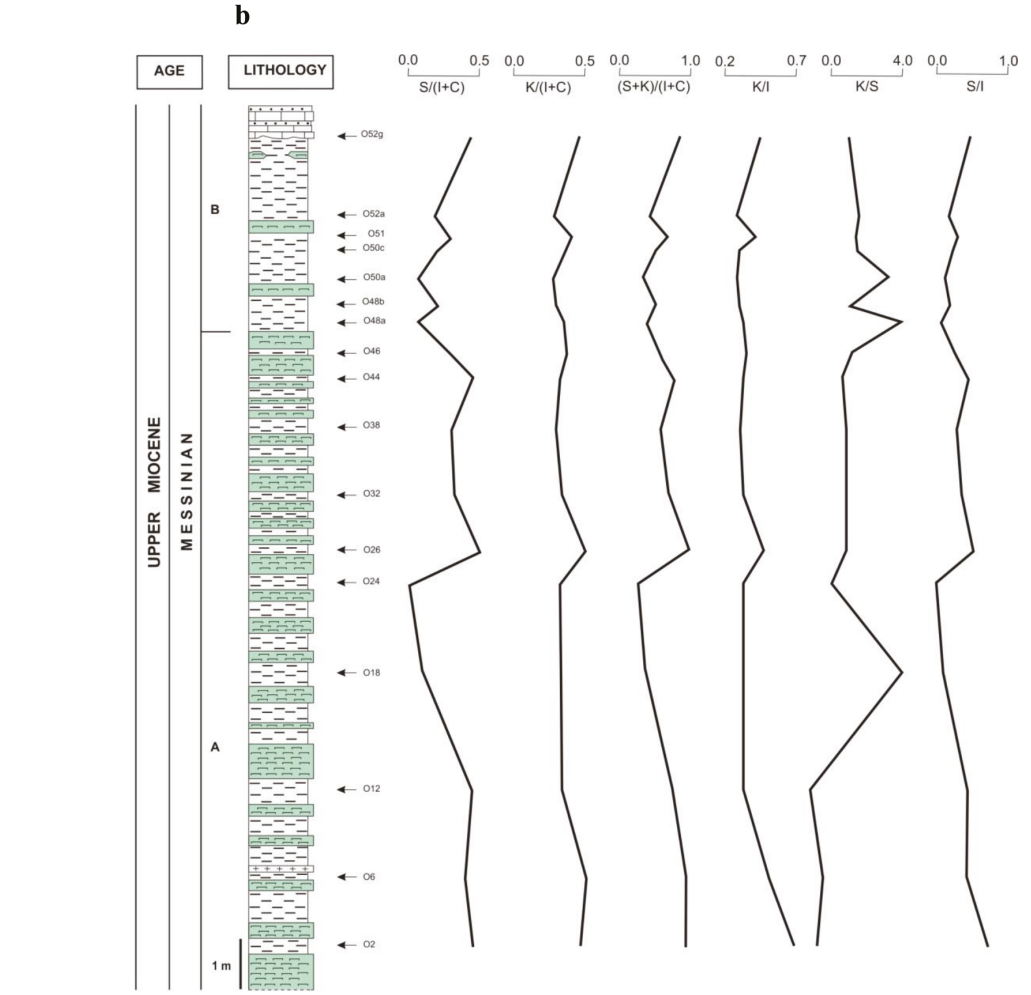

Figure 8. (Continued).

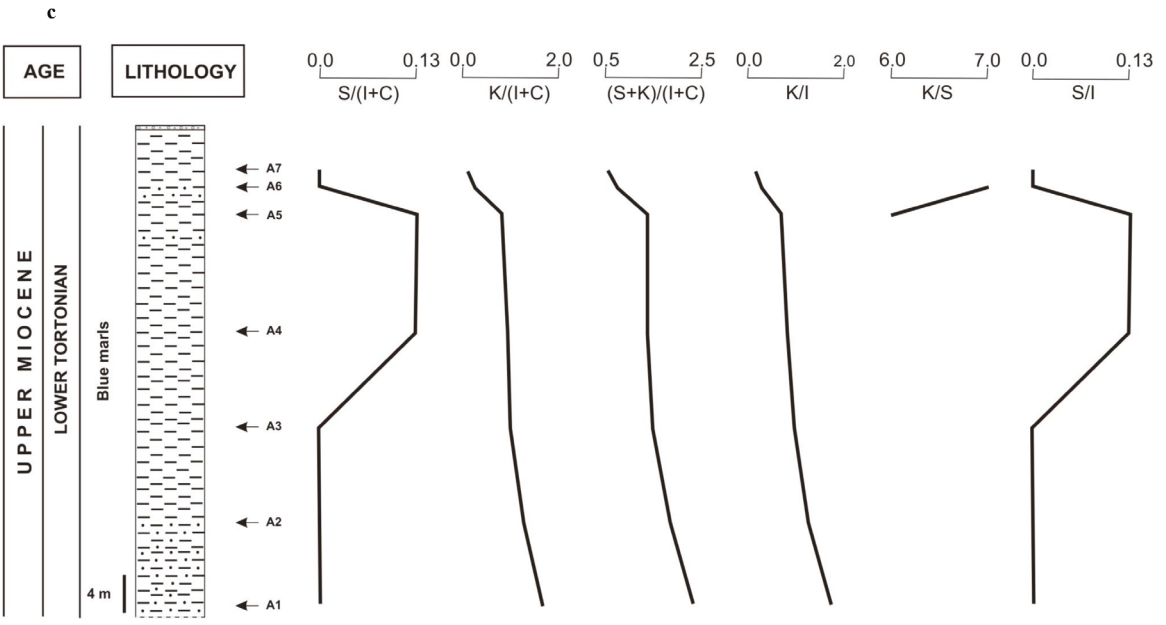

Figure 8. (Continued).

References

Ahlberg A, Olsson I, Šimkevičius P (2003). Triassic–Jurassic weathering and clay mineral dispersal in basement areas and sedimentary basins of southern Sweden. Sediment Geol 161: 15-29.

Aïfa T, Feinberg H, Derder MM, Merabet N (1992). Rotations paléomagnétiques récentes dans le bassin du Chéliff (Algérie). CR Acad Sci II 314: 915-922 (in French).

Aïfa T, Feinberg H, Derder MM, Merabet N (2003). Contraintes magnétostratigraphiques concernant la durée de l'interruption des communications marines en Méditerrannée occidentale pendant le Messinien supérieur. Geodiversitas 25: 617-631 (in French).

Alizai A, Hillier S, Clift PD, Giosan L, Hurst A, Van Laningham S, Macklin M (2012). Clay mineral variations in Holocene terrestrial sediments from the Indus Basin. Quaternary Res 77: 368-381.

Ameur-Chehbeur A (1988). Biochronologie des formations continentales du Néogène et du Quaternaire de l'Algérie. Contribution des micromammifères. PhD, Oran University, Oran, Algeria (in French).

Arab MR, Roure F, Zazoun RS, Mahdjoub Y, Badji R (2015). Source rocks and related petroleum systems of Chelif Basin, (western Tellian domain, north Algeria). Mar Petrol Geol 64: 363-385.

Atif KFT, Bessedik, M, Belkebir L, Mansour B, Saint Martin JP (2008). Le passage Mio-Pliocène dans le bassin du Bas Chélif (Algérie). Biostratigraphie et paléoenvironnements. Geodiversitas 30: 97-116 (in French).

Belhadji A, Belkebir L, Saint Martin JP, Mansour B, Bessedik M, Conesa G (2008). Apports des foraminifères planctoniques à la biostratigraphie du Miocène supérieur et du Pliocène de Djebel Diss (Bassin du Chélif, Algérie). Geodiversitas 30: 79-96 (in French).

Belkebir L (1986). Le Néogène de la bordure nord - occidentale du massif de Dahra (Algérie). Biostratigraphie, Paléoécologie, Paléogéographie. PhD, Provence University, Aix-en-Provence, France (in French).

Belkebir L, Bessedik M, Ameur-Chehbour A, Anglada R (1996). Le Miocène des bassins nord occidentaux d'Algérie : biostratigraphie et eustatisme, in Géologie de l'Afrique et de l'Atlantique Sud, actes Colloques Angers 1994. Elf Aquitaine Éditions, Pau 16: 553-561 (in French).

Belkebir L, Bessedik M, Mansour B (2002). Le Miocène supérieur du Bassin du Bas Chélif : Attribution biostratigraphique à partir des foraminifères planctoniques. Mémoires du Service Géologique de l'Algérie 11: 187-194 (in French).

Bessedik M, Belkebir L, Mansour B (2002). Révision du Miocène inférieur (au sens des anciens auteurs) des dépôts du bassin du bas Chelif (Oran, Algérie). Conséquences biostratigraphiques et géodynamiques. Mémoires du Service Géologique de l'Algérie 11: 167-186.

Biscaye PE (1965). Mineralogy and sedimentation of recent deep-sea clays in the Atlantic Ocean and adjacent seas and oceans. Geol Soc Am Bull 76: 803-832 (in French).

Bizon G, Bizon JJ (1976). Modalités du passage Miocène-Pliocène en Méditerranée: réflexions sur le Messinien. Palaeogeogr Palaeocl 20: 43-46 (in French).

Bockheim JG (1982). Properties of a chronosequence of ultraxerous soils in the Trans-Antarctic Mountains. Geoderma 28: 239-255.

Bolle MP, Adatte T (2001). Palaeocene-early Eocene climatic evolution in the Tethyan realm: clay mineral evidence. Clay Miner 36: 249-261.

Chamley H (1989). Clay Sedimentology. Berlin, Germany: Springer Verlag.

Chamley H (1998). Clay mineral sedimentation in the Ocean. In: Paquet H, Clauer N, editors. Soils and Sediments (Mineralogy and Geochemistry). Berlin, Germany: Springer, pp. 269-302.

Deconinck JF, Chamley H (1995). Diversity of smectite origins in Late Cretaceous sediments; example of chalks from northern France. Clay Miner 30: 365-379.

Delfaud J, Michaux J, Neurdin J, Revet J (1973). Un modèle paléogéographique de la bordure méditerranéenne. Evolution de la région oranaise (Algérie) au Miocène supérieur. Conséquences stratigraphiques. Bulletin de la société d'histoire naturelle d'Afrique du Nord 64: 219-241 (in French).

Delteil J 1974. Tectonique de la chaîne alpine en Algérie d'après l'étude du Tell oriental (Mont de la Mina, Beni Chougrane, Dahra). PhD, Nice University, Nice, France (in French).

Dera G, Pellenard P, Neige P, Deconinck JF, Pucéat E, Dommergues JL (2009). Distribution of clay minerals in Early Jurassic Peritethyan seas: palaeoclimatic significance inferred from multiproxy comparisons. Palaeogeogr Palaeocl 271: 39-51.

Fenet B (1975). Recherche sur l'alpinisation de la bordure septentrionale du bouclier africain à partir de l'étude d'un élément de l'orogenèse nord-maghrébin, les monts du Djebel Tessala et les massifs du littoral oranais. PhD, Nice University, Nice, France (in French).

Garzanti E, Vezzoli G, Lombardo B, Andò S, Mauri E, Monguzzi S, Russo M (2004). Collision-orogen provenance (Western and Central Alps): detrital signatures and unroofing trends. J Geol 112: 145-164.

Grosjean M, van Leeuwen JFN, van der Knaap WO, Geyh MA, Ammann B, Tanner W, Messerli B, Nunez LA, Valero-Garces BL, Veit H (2001). A 22,000 ^{14}C year BP sediment and pollen record of climate change from Laguna Miscanti 23°S, northern Chile. Global Planet Change 28: 35-51.

Guardia P (1975). Géodynamique de la marge alpine du continent africain d'après l'étude de l'Oranie Nord – occidentale (Algérie), relation structurales et paléogéographiques entre Rif externe et le Tell de l'avant pays atlasique. PhD, Nice University, Nice, France.

Hassan AM (2017). Mineral composition and geochemistry of the Upper Cretaceous siliciclastics (Nubia Group), Aswan District, south Egypt: implications for provenance and weathering. J Afr Earth Sci 135: 82-95.

Hu B, Li J, Cui R, Wei H, Zhao J, Li G, Fang X, Ding X, Zou L, Bai F (2014). Clay mineralogy of the riverine sediments of Hainan Island, South China Sea: Implications for weathering and provenance. J Asian Earth Sci 96: 84-92.

Khonde NN, Maurya DM, Chamyal LS (2017). Late Pleistocene-Holocene clay mineral record from the Great Rann of Kachchh Basin, Western India: Implications for palaeoenvironments and sediment sources. Quatern Int 443: 86-98.

Li J, Hua B, Wei H, Zhao J, Zou L, Bai F, Dou Y, Wang L, Fang X (2014). Provenance variations in the Holocene deposits from the southern yellow sea: clay mineralogy evidence. Cont Shelf Res 90: 41-51.

Li J, Liu S, Shi X, Feng X, Fang X, Cao P, Sun X, Wenxing Y, Khokiattiwong S, Kornkanitnan N (2017). Distributions of clay minerals in surface sediments of the middle Bay of Bengal: source and transport pattern. Cont Shelf Res 145: 59-67.

Limmer DR, Köhler CM, Hillier S, Moreton SG, Tabrez AR, Clift PD (2012). Chemical weathering and provenance evolution of Holocene–Recent sediments from the Western Indus Shelf, Northern Arabian Sea inferred from physical and mineralogical properties. Mar Geol 326-328: 101-115.

Liu Z, Wang H, Hantoro WS, Sathiamurthy E, Colin C, Zhao Y, Li J (2012). Climatic and tectonic controls on chemical weathering in tropical Southeast Asia (Malay Peninsula, Borneo, and Sumatra). Chem Geol 291: 1-12.

Mansour B, Bessedik M, Saint Martin JP, Belkebir L (2008). Signification paléoécologie des assemblages de diatomées du Messinien du Dahra sud-occidental (bassin du Chelif, Algérie nord-occidental). Geodiversitas 30: 117-139 (in French).

Mazzola G (1971). Les foraminifères planctoniques du Miocène-Pliocène de l'Algérie nord-occidentale. In: Proceedings of the 2nd Planktonic Conference, Rome, Italy, pp. 787-812 (in French).

Meghraoui M (1982). Étude néotectonique de la région nord-ouest d'El-Asnam : relation avec le séisme du 10 octobre 1980. PhD, Paris VII University, Paris, France (in French).

Meghraoui M (1986). Seismotectonics of the lower Cheleff Basin: Structural Background of the El Asnam (Algeria) earthquake. Tectonics 5: 809-836.

Miao WL, Fan Q, Wei H, Zhang X, Ma H (2016). Clay mineralogical and constraints on late Pleistocene weathering processes of the Qaidam Basin, northern Tibetan Plateau. J Asian Earth Sci 127: 267-280.

Millot G (1970). Geology of Clays. Berlin, Germany: Springer-Verlag.

Mokhtar Samet A (2013). Marnes diatomitiques du Miocène supérieur de la carrière de Ouillis (Bassin du Bas Chelif) : Biostratigraphie et analyse géochimique. MSc, Tlemcen University, Tlemcen, Algeria (in French).

Neurdin-Trescartes J (1992). Le remplissage sédimentaire du bassin Néogène du Chelif, modèle de référence de bassins intramontagneux. PhD, Pau University, Pau, France (in French).

Neurdin-Trescartes J (1995). Paléogéographie du bassin de Chélif (Algérie) au Miocène. Causes et Conséquences. Géologie Méditerranéenne 22: 61-71 (in French).

Perrodon A (1957). Etude géologique des bassins néogènes sublittoraux de l'Algérie occidentale. Bulletin du Service de la Carte géologique d'Algérie 12 (in French).

Rao VP, Rao BR (1995). Provenance and distribution of clay minerals in the sediments of the western continental shelf and slope of India. Cont Shelf Res 15: 1757-1771.

Rateev MA, Gorbunova ZN, Lisitzyn AP, Nosov GL (1969). The distribution of clay minerals in the oceans. Sedimentology 13: 21-43.

Robert C, Chamley H (1991). Development of early Eocene warm climates as inferred from clay mineral variations in oceanic sediments. Global Planet Change 89: 315-331.

Robert C, Kennett JP (1994). Antarctic subtropical humid episode at the Paleocene-Eocene boundary: clay-mineral evidence. Geology 22: 211-214.

Rostási Á, Raucsik B, Andrea Varga A (2011). Palaeoenvironmental controls on the clay mineralogy of Carnian sections from the Transdanubian Range (Hungary). Palaeogeogr Palaeocl 300: 101-112.

Rouchy JM (1982). La genèse des évaporites messiniennes de Méditerranée. Paris, France: Muséum National d'Histoire Naturelle (in French).

Rouchy JM, Caruso A, Pierre C, Blanc-Valleron MM, Bassetti MA (2007). The end of the Messinian salinity crisis: evidences from the Chelif Basin (Algeria). Palaeogeogr Palaeocl 254: 386-417.

Saint-Martin JP (1987). Les formations récifale coralliennes du Miocène supérieur d'Algérie et du Maroc. Aspects paléoécologiques et paléogéographiques. PhD, Aix-Marseille 1 University, Aix-en-Provence, France (in French).

Singer A (1988). Illite in aridic soils, desert dusts and desert loess. Sediment Geol 59: 251-259.

Singh A, Paul D, Sinha R, Thomsen KJ, Gupta S (2016). Geochemistry of buried river sediments from Ghaggar Plains, NW India: multi-proxy records of variations in provenance, paleoclimate, and paleovegetation patterns in the Late Quaternary. Palaeogeogr Palaeocl 449: 85-100.

Tauecchio P, Marks P (1973). The Messinian deposits of the Chelif Basin near El Asnam, Northern Algeria. In: Drooger CW, editor. Messinian Events in the Mediterranean. Amsterdam, the Netherlands: North-Holland, pp. 188-191.

Thiry M (2000). Palaeoclimatic interpretation of clay minerals in marine deposits: an outlook from the continental origin. Earth-Sci Rev 49: 201-221.

Thomas H (1985). Géodynamique d'un bassin intramontagneux. Le bassin du Bas Chelif occidental durant le Mio-Plio-Quaternaire. PhD, Pau et Pays de l'Adour University, Pau, France (in French).

Velde B (1995). Origin and Mineralogy of Clays: Clays and the Environment. New York, NY, USA: Springer-Verlag.

Velde B, Meunier A (2008). The Origin of Clay Minerals in Soils and Weathered Rocks. Berlin, Germany: Springer-Verlag

Wang H, Liu Z, Sathiamurthy E, Colin C, Li J, Zhao Y (2011). Clay mineralogy and elemental geochemistry of river surface sediments in Malay Peninsula and North Borneo. Sci China Earth Sci 54: 272-282.

Weaver CE (1989). Clays, Muds and Shales. Developments in Sedimentology 44. Amsterdam, the Netherlands: Elsevier.